ORIGINAL PAPER

A hitherto unrecognised band in the Raman spectra of silica rocks: influence of hydroxylated Si–O bonds (silanole) on the Raman moganite band in chalcedony and flint (SiO$_2$)

Patrick Schmidt · Ludovic Bellot-Gurlet · Aneta Slodczyk · François Fröhlich

Abstract Chalcedony is a spatial arrangement of hydroxylated nanometre-sized α-quartz (SiO$_2$) crystallites that are often found in association with the silica mineral moganite (SiO$_2$). A supplementary Raman band at 501 cm^{-1} in the chalcedony spectrum, attributed to moganite, has been used for the evaluation of the quartz/moganite ratio in silica rocks. Its frequency lies at 503 cm^{-1} in sedimentary chalcedony, representing a 2 cm^{-1} difference with its position in pure moganite. We present a study of the 503 cm^{-1} band's behaviour upon heat treatment, showing its gradual disappearance upon heating to temperatures above 300 °C. Infrared spectroscopic measurements of the silanole (SiOH) content in the samples as a function of annealing temperature show a good correlation between the disappearance of the 503 cm^{-1} Raman band and the decrease of structural hydroxyl. Thermogravimetric analyses reveal a significant weight loss that can be correlated with the decreasing of this Raman band. X-ray powder diffraction data suggest the moganite content in the samples to remain stable. We propose therefore the existence of a hitherto unknown Raman band at 503 cm^{-1} in chalcedony, assigned to 'free' Si–O vibrations of non-bridging Si–OH that oscillate with a higher natural frequency than bridging Si–O–Si (at 464 cm^{-1}). A similar phenomenon was recently observed in the infrared spectra of chalcedony. The position of this Si–OH-related band is nearly the same as the Raman moganite band and the two bands may interfere. The actually observed Raman band in silica rocks might therefore be a convolution of a silanole and a moganite vibration. These findings have broad implications for future Raman spectroscopic studies of moganite, for the assessment of the quartz/moganite ratio, using this band, must take into account the contribution from silanole that are present in chalcedony and moganite.

Keywords Moganite · Chalcedony · Quartz · Silica rocks · Flint · Heat treatment · Raman band assignment · Silanole (SiOH)

Introduction

Flint is a cretaceous sedimentary silica rock, chiefly composed of chalcedony (Füchtbauer 1988; Cayeux 1929); a spatial arrangement of 50–100 nanometres measuring α-quartz crystallites (Rios et al. 2001). The crystallites align in fibres ranging up to several millimetres or even centimetres in well-crystallised specimens. In flint however, these fibres are shorter and somewhat less organised. Chalcedony contains up to 2 wt% of 'water' that can be differentiated into chemically bound hydroxyl (SiOH) and molecular water (H$_2$O) (Flörke et al. 1982). H$_2$O is mainly held in fluid inclusions and open pores in the rocks (Flörke et al. 1982). Silanole (SiOH) is associated with grain boundaries and defect sites within the quartz crystallites. Numerous Brazil twin interfaces within the crystallites (Cady et al. 1998; Miehe et al. 1984) form another site for

P. Schmidt (✉) · F. Fröhlich
Département de Préhistoire UMR 7194,
Muséum national d'histoire naturelle,
Centre de spectroscopie infrarouge,
CP 57, 57, rue Cuvier, 75231 Paris Cedex 05, France
e-mail: schmidt@mnhn.fr

L. Bellot-Gurlet · A. Slodczyk
Laboratoire de dynamique,
interactions et réactivité (LADIR) UMR 7075,
CNRS and UPMC (Université Pierre et Marie Curie, Paris 6),
4 Place Jussieu, 75252 Paris Cedex 05, France

the integration of silanole (Graetsch et al. 1985). The hydroxylation of SiO_4 tetrahedra inhibits the formation of bridging Si–O–Si bonds resulting in non-bridging Si–OH that cause a supplementary Q_3 peak in ^{29}Si CP-MAS-NMR of chalcedony (Graetsch et al. 1994). Using FT-IR spectroscopy, Schmidt and Fröhlich (2011) showed that non-bridging Si–OH causes a supplementary band in the mid-infrared at 555 cm^{-1}. This band disappears gradually upon heating between 300 and 600 °C, showing a good correlation with the loss of silanole. The reduction of the band's intensity is caused by the formation of new bridging Si–O–Si after the evacuation of hydrogen.

Another silica polymorph, commonly associated with chalcedony, is moganite (Flörke et al. 1976; Flörke et al. 1984). The monoclinic moganite lattice can be described as a framework of $(10\bar{1}1)$ left- and right-handed quartz lamellae that alternate on the unit cell scale (Miehe et al. 1986; Miehe and Graetsch 1992). The structure has therefore been associated with $(10\bar{1}1)$ Brazil law twin boundaries in chalcedony and flint (Miehe et al. 1984). Heaney and Post (1992) found moganite to be associated with a large number of microcrystalline silica rocks. In such quartz/moganite mixtures, the mineral causes supplementary peaks in the powder diffraction pattern (Heaney and Post 1992; Flörke et al. 1984) and a band between 501 and 503 cm^{-1} in the Raman spectrum (Kingma and Hemley 1994; Heaney et al. 2007). Kingma and Hemley (1994) assigned the Raman band to four-membered rings of SiO_4 tetrahedra in the moganite structure. The frequency of the band shifts to lower wavenumbers with rising temperature, passing through a plateau between 296 and 316 °C (Heaney et al. 2007), and X-ray powder diffraction data indicate a displacive monoclinic to orthorhombic phase transition between these temperatures (Heaney and Post 2001). Apart from the phase transition, the thermal stability of moganite ranges up to 900–1,000 °C where it transforms into cristobalite (Flörke et al. 1984; Miehe and Graetsch 1992). Moganite has not been found in rocks dating from before 400 Ma (Moxon and Rios 2004), and Rodgers and Cressey (2001) reported the mineral to be a meta-stable intermediary step in the opal-A to quartz maturation that transforms into chalcedonic quartz over extended time periods.

Due to a supplementary band at 501 cm^{-1}, Raman spectroscopy has proven a rapid non-destructive means of moganite detection in silica rocks. The ratio between this band and the adjacent quartz band at 464 cm^{-1} has been used for evaluating the rock's moganite content (Götze et al. 1998; Rodgers and Hampton 2003; Nash and Hopkinson 2004; Bustillo et al. 2010). We present here a study showing the actually observed band in chalcedony to be more complicated and reveal the behaviour of this Raman band upon heat treatment. The study aims in creating a better understanding of the different factors that contribute to the temperature-dependent evolution of the Raman 'moganite signal'.

Materials and methods

Samples

Five specimens of cretaceous flint and one sample of almost pure moganite from Gran Canaria (ES) were analysed. The moganite sample was identified as such using infrared and Raman spectroscopy. All analysed flint samples consist of length-fast chalcedony. This was verified by polarised light microscopy using 30 μm thin sections of each sample. No traces of opal-CT were found during X-ray analyses. Sample numbers and descriptions are summarised in Table 1.

Table 1 Sample descriptions and annealing temperatures

Analysis type	Sample number	Description	Annealing temperatures (°C)
Powder, measured ex situ, IR, Raman, XRD	TR-S-01	Turonian black flint, consisting of length-fast (LF) chalcedony. North of Tours, France	200, 250, 300, 350, 400, 450, 500, 550, 600
Powder, measured ex situ, IR, Raman	GP-S-01	Upper cretaceous brown flint, consisting of LF chalcedony. *Le grand Pressigny*, France	110, 200, 250, 300, 350, 400, 450, 500, 550, 600, 700
Polished section, heating stage, IR, Raman, TG	PS-09-04	Coniacian black flint, consisting of LF chalcedony. Étretat, France. Sample thickness: 545 ± 5 μm	100, 150, 200, 250, 300, 350, 400, 450, 500, 550, 600, 700, 800
Polished section, heating stage, Raman	PS-S-02	Turonian brown flint, consisting of LF chalcedony. East of Tours, France. Sample thickness: 690 ± 10 μm	100, 150, 200, 250, 300, 350, 400, 450, 500, 550, 600, 700
2 thin sections, measured ex situ, Raman	R-GE-Cal	Botryoidal sedimentary LF chalcedony from a cavity in flint. From upper cretaceous chalk, *plage d'Étretat*, France	Unheated, 700
Raman	GC-11-01	White powdery joint filling material from ignimbrite. Almost pure moganite, Gran Canaria, Spain	Unheated

Used instruments and settings

Raman spectra were acquired between 100 and 800 cm^{-1} using a Horiba Jobin Yvon HR800 spectrometer equipped with edge filters. The exciting wavelength was the 458 nm line of an Ar$^+$ laser that, in combination with a 1,800 lines/mm grating, results in a spectral resolution of ≈ 1 cm^{-1}. Measurements for the determination of precise band frequencies were carried out with a 2,400 lines/mm grating, resulting in a spectral resolution of ≈ 0.5 cm^{-1}. Spectrometer calibration was set using the 520.5 cm^{-1} band of a Si crystal. A $10\times$ objective, producing an exciting spot of approximately 10 μm, was used for spectral acquisition on powders. Heating-stage (Linkam TS1500) experiments were carried out with a $50\times$ long working distance objective. Spectra were acquired during 4–6 min.

Infrared spectra were acquired with a Bruker VECTOR 22 FTIR spectrometer by means of attenuated total reflectance (ATR) and direct transmission. ATR spectra were recorded between 1,400 and 400 cm^{-1} with a resolution of 2 cm^{-1}. Transmission spectra were acquired between 4,800 and 4,200 cm^{-1} with a resolution of 8 cm^{-1}.

The dynamical weight loss as a function of annealing temperature and time was studied using a SETARAM Setsys Evolution thermo balance. Approximately 70 mg of powder (grain size <1 μm) were used. The use of a platinum crucible and helium atmosphere increased the heat transfer significantly and consequently allowed for better measurement accuracy.

Powder diffractograms were recorded between $2\vartheta = 2°$ and $35°$ using a PANalytical X'Pert Pro MPD diffractometer (using the K_α line of a Cu anode, no incident beam monochromator). The sample holder was in constant rotation during the analysis.

Experimental

Raman measurements

The comparison of raw spectra of pure moganite and flint is based on two spectra acquired with the 2,400 lines/mm grating. Moganite and chalcedony spectra were acquired one directly after the other, maintaining the same spectrometer calibration and parameters.

All other spectra in this study were acquired using the 1,800 lines/mm grating. Two polished thin sections were cut from sample R-GE-Cal, one from the unheated sample and one from the sample after annealing at 700 °C during 6 h in a Thermolyne 47900 electrical furnace with free access to oxygen.

For measurements on powder, the samples TR-S-01 and GP-S-01 were each broken into fragments weighing approximately 4 g. Each fragment was heated during 6 h to a different temperature between 100 and 700 °C. The fragments were then ground and screened with a mesh width of 40 μm. Using a light microscope, the average grain size of the powders was estimated to ≈ 4 μm.

For heating stage measurements, the samples PS-S-02 and PS-09-04 were cut into thin slabs and diamond-polished on both sides (for sample thicknesses see Table 1). Two different ramps were programmed for the two samples. Sample PS-S-02 was heated to the first annealing temperature (Table 1) where a spectrum was acquired. The temperature was held for 30 min, and a second spectrum was acquired before the sample was heated to the next higher temperature. A different ramp was programmed for sample PS-09-04. The section was heated to the first annealing temperature (Table 1) where a spectrum was acquired. The heating stage was then cooled down to 40 °C, and a 'cold' spectrum was acquired before the sample was heated to the next higher temperature. This protocol allows for the comparison between in situ spectra acquired at high temperatures and quenched spectra (ex situ) acquired directly after heating. Another fragment of sample PS-09-04 was rapidly (50 °C/min) heated to 450 °C in the heating stage and held at this temperature during 6 h. A spectrum was acquired every minute as soon as this temperature was reached. After the first 15 min of this temperature plateau, spectra were acquired every 5 min and after 1 h, every 30 min. This protocol allows for the evaluation of the reaction kinetics.

Infrared measurements

In order to investigate the sample's silanole content after heating, a part of each polished section was broken off for analysis in the near infrared. The hydroxyl content was directly measured through the Si–OH combination band near 4,500 cm^{-1} (Scholze 1960; Flörke et al. 1982). Annealing temperatures for infrared measurements were identical with the Raman measurements (Table 1). Infrared ATR spectra were acquired on the powders already analysed by Raman spectroscopy.

Thermogravimetric analysis (TGA)

The variation of mass as a function of time was determined for sample PS-09-04. The sample was wet ground for 30 min, and the very finest part of the powder was separated by decantation. The so-obtained powder has an estimated grain size significantly smaller than 0.5 μm. This powder was first heated to 150 °C and held at this temperature during 4 h in order to eliminate loosely held molecular water adsorbed during grinding. The sample was then rapidly heated to 450 °C, and the temperature was

held during 6 h in order to observe the weight loss as a function of time. The so-observed reaction kinetics of the weight loss at 450 °C can be attributed to the evaporation of SiOH.

X-ray powder diffraction

In order to evaluate the moganite content of one of the samples by a complementary technique, two powders obtained from TR-S-01 (grain size ≈ 4 μm) were analysed by XRD, one powder before heating and one after annealing at 600 °C during 6 h. The two powders were each divided into 3 equal parts that were treated separately in order to minimise orientation effects during the preparation. The comparison of the intensities of the moganite peaks at 4.45, 3.11 and 2.88 Å before and after heat treatment allows for verifying if the moganite content of the samples is either lost or remains stable upon heat treatment at 600 °C.

Raman and infrared signal processing and error bars

The ratio between the Raman band intensities near 503 cm^{-1}, and the 464 cm^{-1} quartz band was calculated in order to investigate the temperature-dependant behaviour of the moganite Raman band. The baseline for the intensity measurements was a straight line drawn between the two lowest points on either side of the two bands. Band intensities for room temperature spectra are linear absorptions, band intensities of in situ spectra were measured as the ratio between the bands' heights and widths. These heights and widths were extracted from best fit models of the spectra, using Lorentzian functions. Error bars were estimated by repeating spectral acquisition 5 times on different parts of one powdered sample. The maximal deviation from the arithmetic mean of the obtained values was used for error bars. These error bars were found to be appropriate for powder samples and polished sections. Relative infrared intensities at 555 cm^{-1} are expressed through the ratio between the band's intensity and the intensity of a strong lattice band that was found not to vary with temperature (1,166 cm^{-1}). Analysis parameters, error bars and baselines for the infrared measurements are described in detail in the study by Schmidt and Fröhlich (2011).

Results

Comparison between the spectra of pure moganite and chalcedony

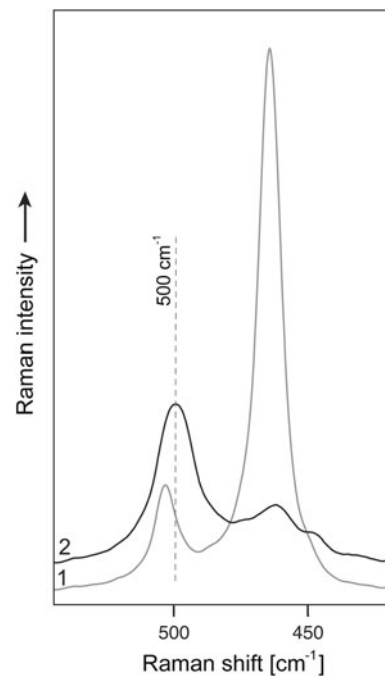The moganite-specific Raman band in sample CG-11-01 was found at 500 cm^{-1}. The band in our chalcedony

Fig. 1 Comparison of room temperature Raman spectra of *1* PS-S-02 and *2* GC-11-01. Spectra displaced vertically. Spectral resolution was ≈ 0.4 cm^{-1}. Both spectra were acquired directly one after the other using the same spectrometer calibration and settings. The pure moganite sample GC-11-01 shows a band at 500 cm^{-1}, whereas the chalcedony sample PS-S-02 shows a band at 503 cm^{-1}. This 3 cm^{-1} frequency shift indicates the different nature of both bands

samples was found at 503 cm^{-1} (Fig. 1). The 3 cm^{-1} difference between the moganite and chalcedony bands, using the same parameters, is significant and shows their different nature. The band was found at 503 cm^{-1} in all other analysed flint samples and will be referred to as 503 cm^{-1} band hereafter.

Room temperature Raman and infrared spectra of annealed flint samples

The Raman spectrum of the unheated flint sample GP-S-01 shows a strong quartz band at 464 cm^{-1} and the additional band at 503 cm^{-1} (Fig. 2). The latter is missing in the spectrum acquired after annealing at 700 °C during 6 h. The band also disappears progressively upon high temperatures in the two powder samples. The evolution of the 503/464 cm^{-1} ratio as a function of annealing temperature is shown in Fig. 3. The value of the ratio decreases from 300 °C upwards and seems to plateau between 550 and 600 °C for TR-S-01 (square in Fig. 3). The plot of the ratio in GP-S-01 shows a higher dispersion but the same trend of the 503 cm^{-1} band to decrease at higher temperatures is obvious (triangle in Fig. 3). ATR infrared spectra acquired on the same powders show a similar trend. Figure 4 is a plot of the intensity of the infrared 555 cm^{-1} band as a
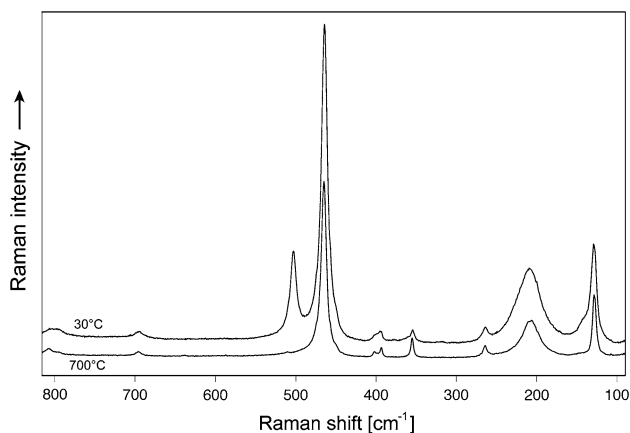
Fig. 2 Two Raman spectra of sample PS-GE-Cal. The upper spectrum was acquired before heat treatment and the lower spectrum after annealing at 700 °C during 6 h. The 503 cm^{-1} Raman band disappeared almost completely after heat treatment. Spectral acquisition was 16 min
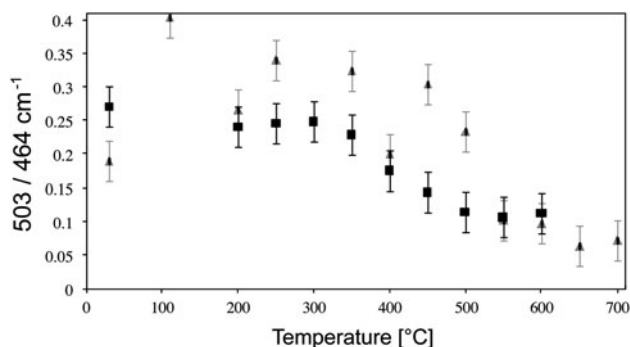

Fig. 4 Plots of the infrared 555/1,166 cm^{-1} absorption index against annealing temperature, *square* TR-S-01, *triangle* GP-S-01. The absorption index is obtained by dividing the measured absorption at 555 cm^{-1} by a strong lattice band that was found not to vary with temperature. ATR spectra for the absorption measurements were acquired on the same sample powders as for Raman measurements shown in Fig. 5

Fig. 3 Plots of the value of the Raman 503/464 cm^{-1} ratio against annealing temperature, *square* TR-S-01, *triangle* GP-S-01. Both plots show the relative reduction of the 503 cm^{-1} band's intensity after heat treatment. Spectra for the measurements were acquired at room temperature after heat treatment

Fig. 5 Comparison between in situ Raman spectra acquired at different temperatures of PS-S-02 (*RT* room temperature). Spectra displaced vertically. The absolute band intensities in this figure were modified for better readability. For measurements of the relative band intensities, see Fig. 7a. The frequency shift and band-broadening at elevated temperatures can be observed

function of the annealing temperature. As for the Raman measurements, the intensity of the ATR 555 cm^{-1} band decreases from 300 °C upwards (square in Fig. 4). In the case of GP-S-01, the values of the band's intensity show higher dispersion but the decrease from 500 °C upwards is evident (triangle in Fig. 4). The higher dispersion of results from sample GP-S-01 may be related to inner sample heterogeneity. The comparison of Figs. 3 and 4, however, indicates a similar temperature-dependent evolution of the 503 cm^{-1} Raman band and the 555 cm^{-1} infrared band.

Heating-stage experiments on flint

Frequency shift

Figure 5 shows the comparison of 5 in situ spectra of PS-S-02 acquired at different temperatures. Both observed Raman
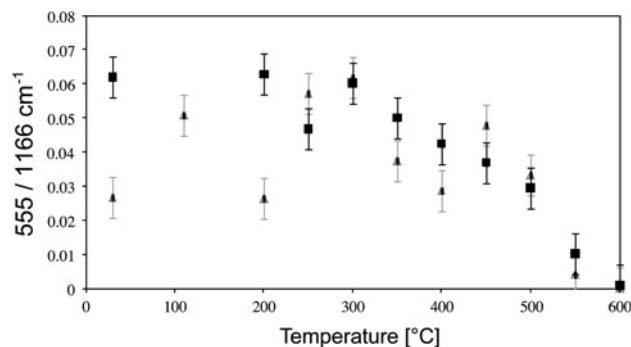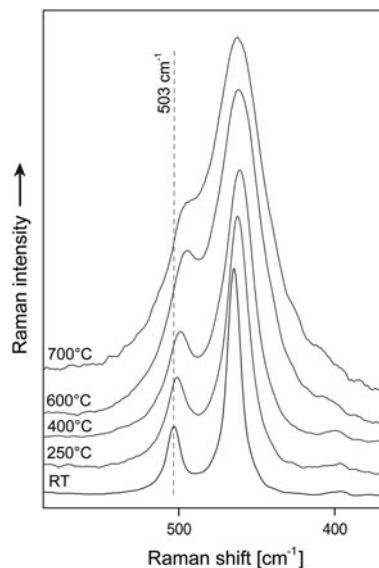
bands (503 and 464 cm^{-1}) shift to lower wavenumbers at elevated temperatures. This shift was already observed (Heaney et al. 2007) in pure moganite from Gran Canaria (ES). Figure 6 is a plot of the position of these bands against annealing temperature from in situ recorded spectra of sample PS-S-02. Both bands shift to lower wavenumbers upon rising temperatures. The frequency shift is greater for the 503 cm^{-1} band (6 cm^{-1} against 3.5 cm^{-1} for the quartz band). Both bands shift to lower wavenumbers until 500–600 °C. A plateau between 296 and 316 °C, as
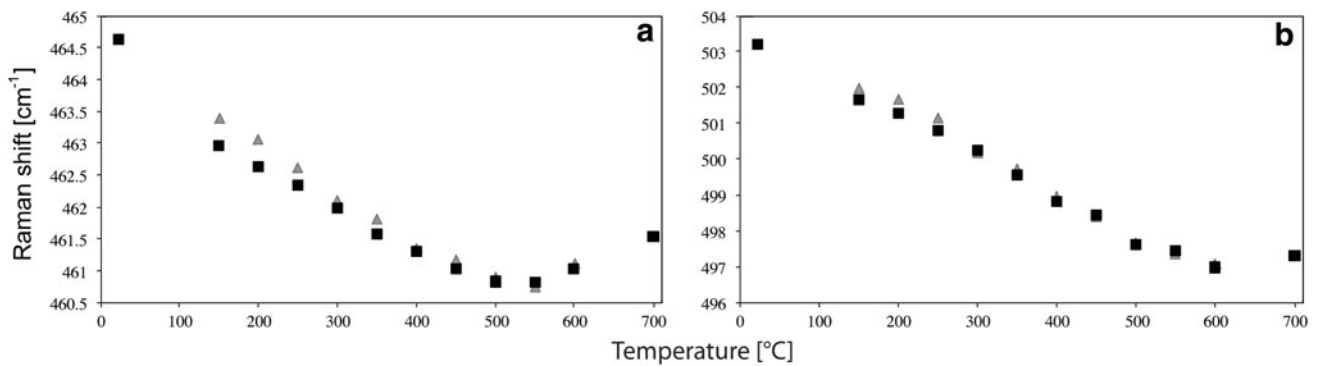
Fig. 6 Plots of the position of the Raman 464 cm^{-1} (**a**) and 503 cm^{-1} (**b**) bands against annealing temperature in sample PS-S-02 (first spectrum at plateau *square*, second spectrum *triangle*, for explanation see Sect. 2.3.1). Spectra for the measurements were described by Heaney et al. (2007), indicating the moganite phase transition cannot be observed in sedimentary LF chalcedony. After a turning point around these temperatures, the shift becomes less important. Concerning the difference between the first and second spectra (time difference of 30 min) taken at an annealing temperature, the Raman shift values are slightly different, indicating a time-dependent evolution. Bands in the first spectra are located at slightly higher wavenumbers than bands from spectra recorded after 30-min annealing time. However, this time-dependent evolution seems to be included in the estimated error of the measurements (±0.5 cm^{-1}, based in the spectrometer's resolution) and cannot be discussed here.

acquired in situ using a heating stage. *Error bars* for the obtained values are missing for better readability. The error can be estimated based on the spectrometer's resolution and is expected to be ±0.5 cm^{-1}

Band intensities

The ratio between the 503 cm^{-1} Raman band and the adjacent quartz band of in situ spectra shows a

temperature-dependent evolution (Fig. 7a). However, the results of the band fitting seem to be ambiguous, for the plots of in situ measurements show less detail than the ones resulting from room temperature measurements (Fig. 5). The values seem to increase until 250 °C and their reduction becomes apparent only from 500 °C upwards. The differences of these plots with room temperature spectra are illustrated by the comparison between the values of in situ and ex situ measurements of PS-09-04 [compare circle in Fig. 7a (in situ) with square in Fig. 7b (ex situ)]. The figure shows the differences between the two types of spectra. Room temperature spectra do not show the increase of the values between 30 and 250 °C. This difference is likely to be caused by a temperature-dependent variation of the Raman tensors of the two bands. In this case, the gain of the band's intensity can be attributed to an increasing Raman tensor with rising temperatures. The turning point at 250 °C is caused by the beginning of the
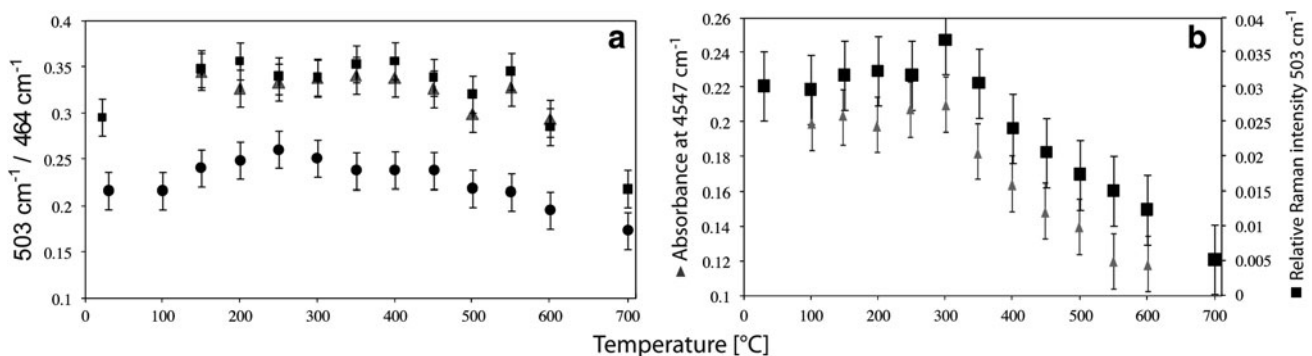

Fig. 7 a Plot of the relative intensity of the 503 cm^{-1} Raman band against annealing temperature. For the calculation of band intensities from in situ spectra, see Sect. 2.4. PS-S-02 (first spectrum at plateau *square*, second spectrum at plateau *triangle*, for explanation see Sect. 2.3.1.) and PS-09-04 (*circle*). Spectra for the measurements were acquired in situ using a heating stage. **b** Plots of the infrared Si–OH absorption at 4,547 cm^{-1} (*triangle*) and the relative intensity of the

Raman band at 503 cm^{-1} (*square*) against annealing temperature of PS-09-04. Sample thickness was 545 ± 5 μm. *Scale* to the *left* of the graph: IR absorption at 4,547 cm^{-1} (*triangle*), *scale* to the *right*: relative Raman intensity of the 503 cm^{-1} band (*square*). The starting temperature of the reduction of the IR and Raman bands is 300 °C and the pace of their reduction shows their correlation

band's intensity loss. This variation of the Raman tensor at higher temperatures partly masks the phenomenon of the 503 cm^{-1} band's reduction.

Comparison of flint Raman spectra with NIR spectra

Figure 7b shows the plot of the intensity decrease in the 503 cm^{-1} Raman band, as determined by the PS-09-04 ex situ measurements, compared with the reduction of silanole as measured by infrared absorption on the same polished section. This comparison cannot be made between in situ Raman measurements and ex situ infrared measurements, for the temperature-dependent variation of the Raman tensor modifies the shape of the plots. The plots of the intensity of the Si–OH absorption and the relative intensity of the 503 cm^{-1} band show an identical pace, indicating a good correlation between the Raman band and the silanole content of the sample.

Diffraction data of flint

A comparison between the diffractograms acquired before and after heat treatment is shown in Fig. 8. The sample's diffraction pattern shows additional weak moganite peaks (labelled with "M"), indicating the presence of traces of moganite (<5 %) in the chalcedony sample. These peaks remain unchanged after annealing. Thus, the X-ray moganite signal remains stable after heat treatment at 600 °C.
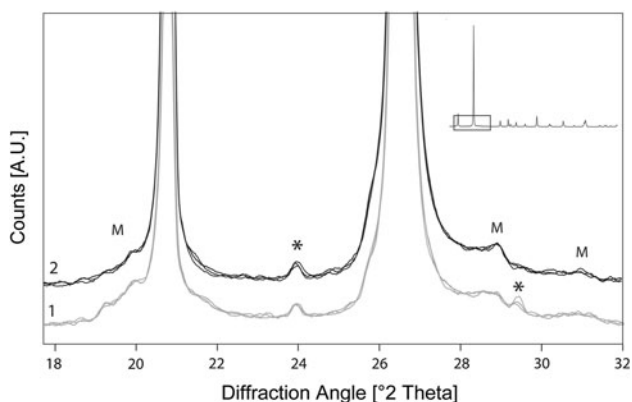

Fig. 8 Comparison between the regions of the X-ray powder diffractograms (K_α line of a Cu anode with 1.54 Å, no incident beam monochromator) of TR-S-01, showing the weak moganite peaks before *1* and after heat treatment at 600 °C *2*. The three superposed diffractograms correspond to the three measurements described in Sect. 2.3.4. Diffractograms displaced vertically. Moganite peaks are labelled "M", and other impurities are labelled *asterisk*. The diffractogram in the *upper right corner* shows the location of this figure on the complete chalcedony diffractogram. Intensities of the quartz peaks were normalised in the two presented diffractograms 1 and 2, so that the comparison of the moganite peak intensities is significant. This comparison shows the X-ray moganite signal to remain stable after heat treatment

Raman spectra acquired on the same two powders showed the reduction of the 503 cm^{-1} band (Fig. 3). The comparison between X-ray and Raman data suggests the 503 cm^{-1} band reduction to be independent of the sample's moganite content.

Thermogravimetric analysis and reaction kinetics in flint

The results of the TG measurements show the weight loss of PS-09-04 as a function of annealing time (Fig. 9a). The mass lost at the first heating step at 150 °C can be attributed to molecular water held between grains and water adsorbed on their surface. However, the total measured quantity of weight loss in this powder is significantly higher than that in coarser powders. This is because the artificially created large specific surface of the particles allows for a stronger surface hydration. The second weight loss at 450 °C can be attributed to the loss of silanole, for most of the molecular water was already lost at 150 °C (Flörke et al. 1982; Graetsch et al. 1985). The obtained SiOH weight loss can be expected to show the same reaction kinetics in the studied fine grained powder as in coarser powders, for it depends on the strength and stability of the Si–OH bond. Figure 9b shows a comparison between Raman data of the 503 cm^{-1} band's reduction and the TG measurement of the silanole loss at 450 °C (second heating step from Fig. 9a). Both the TG curve and the plot of the Raman values show the strongest reaction during the first hour of heating at 450 °C and a very good superposition. This result suggests a strong correlation between the reaction kinetics of the 503 cm^{-1} band's reduction and the reaction kinetics of silanole loss in the sample.

As stated earlier, the total amount of lost weight is not significant for the study of chalcedony at this very small grain size of the used powder. In order to quantify the total weight loss in the sample, a coarser grained powder (≈ 10 μm) was heated until 1,000 °C. The TG analysis of this coarser grained powder shows the totally lost mass (H_2O and SiOH) of the sample to be approximately 1.2 wt%. This value is in accordance with the previously published (Flörke et al. 1982; Schmidt et al. 2011) total 'water' content of LF chalcedony.

Discussion

The Raman band observed in the present study of sedimentary LF chalcedony was found at 503 cm^{-1}. The Moganite Raman band, assigned to crystal vibrations (Kingma and Hemley 1994), was previously described at 501 cm^{-1} (Heaney et al. 2007; Rodgers and Cressey 2001) and at 502 cm^{-1} (Götze et al. 1998). We found the band at
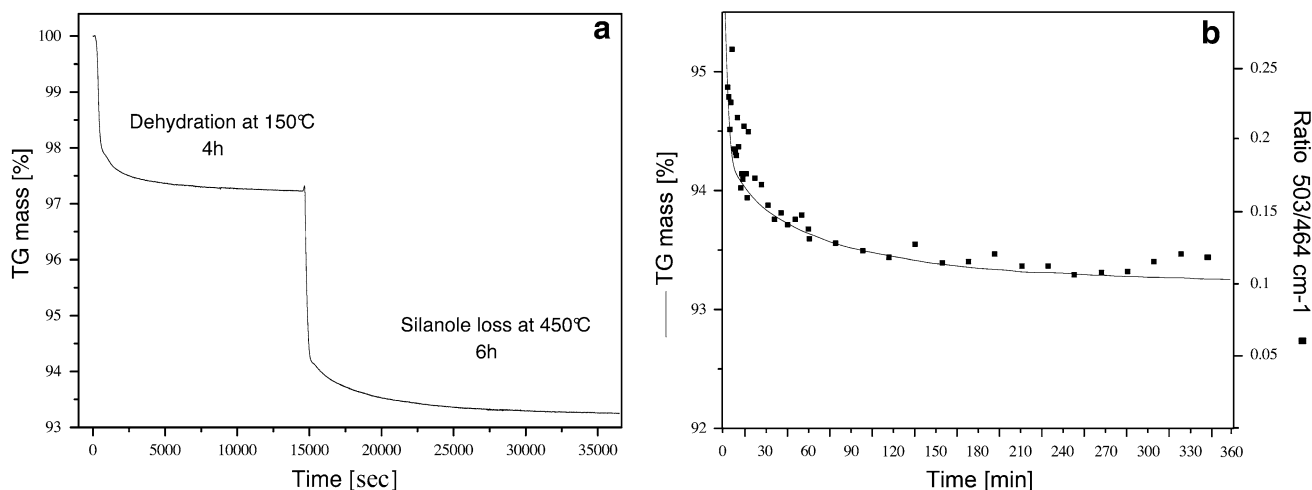
Fig. 9 **a** TG *curve* of a very fine grained powder (<0.5 μm) of PS-09-04. The curve shows the two heating steps at 150 and 450 °C. Due to the very small grain size, the value of weight loss is not significant for the study of LF chalcedony. Only reaction kinetics of the observed weight losses are significant. Further descriptions in the text. **b** Superposition of the plot of the relative reduction of the 503 cm^{-1} Raman band as a function of time upon annealing at 450 °C (*square*), and the TG *curve* showing the weight loss attributed to the loss of SiOH as a function of time at the same temperature (—). The beginning of the graph corresponds to the time the sample reached 450 °C. Both *curves* show a good correlation indication that reaction kinetics of the two phenomena is identical

500 cm^{-1} in the pure moganite sample from Gran Canaria (ES). A difference of 2 to 3 cm^{-1} in absolute position might be insignificant in view of the different instruments or calibration used during our study and previous works. However, spectral acquisitions on a chalcedony and a moganite sample, one after the other, using the same spectrometer calibration and settings clearly reveal the different nature of the bands in pure moganite and chalcedony (Fig. 1). We therefore reveal the existence of two bands at proximate wavenumbers in the Raman spectra of chalcedony.

A supplementary indication for the unrelatedness of the 503 cm^{-1} band in LF chalcedony and the moganite content of the samples comes from our powder diffraction data. X-ray suggests a weak moganite content of a few per cent (<5 %) in the chalcedony sample. The observed Raman band in the same sample is significantly more intense than a band that would be caused by 5 % moganite (if the observed 503 cm^{-1} band was caused by moganite, its intensity would indicate >50 %, based on the calibration curve given in Götze et al. 1998). Additionally, the diffractograms acquired before and after heat treatment suggest that there is no correlation between the Raman band's thermal behaviour and the moganite content of the samples (Fig. 8). The thermal stability of moganite is in accordance with data from previous workers (Flörke et al. 1984; Miehe and Graetsch 1992) who suggest the moganite structure to remain stable until at least 900 °C. The unrelatedness of the observed Raman band with moganite is further corroborated by the in situ Raman band shift at elevated temperatures in the LF chalcedony spectra (Fig. 6). The band shift does not show any sign of a phase transition as it is characteristic for pure moganite from Gran Canaria (ES) (Heaney et al. 2007). Also, a loss of the band's intensity was not noticed during the study performed by Heaney et al. (2007), further suggesting a difference between the Raman band of pure moganite from Gran Canaria and the Raman band observed in LF chalcedony. The measurement of the reaction kinetics of the chalcedony Raman band's reduction indicates that the band is correlated with a TG weight loss (Fig. 9b). Given that the conversion from moganite to quartz corresponds to a reconstructive phase transition, which does not involve the departure of mass, the reduction of the 503 cm^{-1} Raman band in LF chalcedony cannot be assigned to the loss of moganite that transforms to quartz at elevated temperatures. All these results strongly indicate that the observed 503 cm^{-1} Raman band in LF chalcedony is not, or not uniquely, caused by the moganite content of the samples.

Concerning the assignment of the 503 cm^{-1} Raman band, the thermal behaviour of the band gives clear indication of its relation with silanole groups. The present study shows that the 503 cm^{-1} Raman band disappears gradually upon heat treatment from 300 °C upwards. Upon heat treatment, this chalcedony Raman band shows a very similar behaviour with the 555 cm^{-1} infrared band of sedimentary LF chalcedony that has previously been assigned to non-bridging Si–O vibrations that result from silanole in chalcedony (Schmidt and Fröhlich 2011). The intensities of both bands decrease at temperatures above 300 °C (compare Figs. 3, 4). In addition to the concomitant decrease in the 503 cm^{-1} Raman and 555 cm^{-1} infrared

bands upon heating, the reaction kinetics of the Raman band's reduction at 450 °C is correlated with the loss of silanole (Fig. 9b). Fukuda and Nakashima (2008), using in situ infrared measurements of chalcedony, found a very similar evolution of the silanole content at high temperature (disappearance during the first hour of heating). The comparison between the 503 cm^{-1} Raman band's reduction and the loss of silanole as determined through NIR spectroscopy further indicates a good correlation between the intensity of the band and the silanole content of the samples after heat treatment (Fig. 7b).

It seems therefore that two Raman bands may lie very near to each other in the spectra of chalcedony, a moganite band and another, hitherto unrecognised, band at a slightly higher wavenumber. The two bands may interfere in moganite-rich chalcedony and form a composite band. These two bands are [1] a band caused by a moganite crystal vibration at 500–501 cm^{-1}, as observed during the study of pure moganite from Gran Canaria (this band is not lost during heat treatment) and [2] a supplementary band at 503 cm^{-1} caused by the silanole content of the samples (this band is lost upon heat treatment). Band [2] seems thus to correspond to Si–O vibrations in non-bridging Si–OH. The absence of a bond with a second Si (as in Si–O–Si) can account for the higher frequency of such a Si–OH vibration when compared to bridging Si–O–Si. The existence of two Raman active bands at nearly the same wavenumber is analogous to infrared spectroscopy. The 555 cm^{-1} infrared band, assigned to free Si–O vibrations (in Si-OH) (Schmidt et al. 2011; Schmidt and Fröhlich 2011), has a very similar position as the specific infrared band caused by the moganite lattice near 570 cm^{-1} (Flörke et al. 1976; Miehe and Graetsch 1992).

Conclusion

These findings have broad implications for future Raman spectroscopic studies of moganite in silica rocks. In the past, the 503 cm^{-1} band might have been mistakenly interpreted as moganite signal. The future Raman assessment of the quartz/moganite ratio must take into account the contribution from free Si–O vibrations of silanole that are present in chalcedony and moganite. Thus, in order to conduct studies of the stability of moganite over time or the moganite content in silica rocks, the assessment of the relative intensity of the 503 cm^{-1} band has to be interpreted cautiously.

References

Bustillo MA, Pérez-Jiménez JL, Alonso-Zarza AM, Furio M (2010) Moganite in the chalcedony varieties of continental cherts (Miocene, Madrid Basin, Spain). In: Conference on micro-Raman spectroscopy and luminescence studies in the earth and planetary sciences (CORALS II), held 18–20 May 2011 in Madrid, Spain., Madrid (Spain). LPI Contribution, p 16

Cady SL, Wenk HR, Sintubin M (1998) Microfibrous quartz varieties: characterization by quantitative X-ray texture analysis and transmission electron microscopy. Contrib Miner Petrol 130(3):320–335

Cayeux L (1929) Les Roches sédimentaires de France. Roches siliceuses, vol 1. Impr. Nat., Paris

Flörke OW, Jones JB, Schmincke HU (1976) A new microcrystalline silica from Gran Canaria. Z Kristallogr 143:156–165

Flörke OW, Köhler-Herbertz B, Langer K, Tönges I (1982) Water in microcrystalline quartz of volcanic origin: Agates. Contrib Miner Petrol 80(4):324–333

Flörke OW, Flörke U, Giese U (1984) Moganite, a new microcrystalline silica-mineral. Neues Jahrbuch für Mineralogie Abhandlungen 149(3):325–336

Füchtbauer H (1988) Sedimente und Sedimentgesteine, 4th edn. Schweizerbart, Stuttgart

Fukuda J, Nakashima S (2008) Water at high temperatures in a microcrystalline silica (chalcedony) by in-situ infrared spectroscopy: physicochemical states and dehydration behavior. J Mineral Petrol Sci 103:112–115

Götze J, Nasdala L, Kleeberg R, Wenzel M (1998) Occurrence and distribution of "moganite" in agate/chalcedony: a combined micro-Raman, Rietveld, and cathodoluminescence study. Contrib Miner Petrol 133(1):96–105

Graetsch H, Flörke OW, Miehe G (1985) The nature of water in chalcedony and opal-C from Brazilian agate geodes. Phys Chem Miner 12(5):300–306

Graetsch H, Topalovic I, Gies H (1994) NMR spectra of moganite and chalcedony. Eur J Mineral 6(4):459–464

Heaney PJ, Post JE (1992) The widespread distribution of a novel silica polymorph in microcrystalline quartz varieties. Science 255(5043):441–443. doi:10.1126/science.255.5043.441

Heaney PJ, Post JE (2001) Evidence for an I2/a to Imab phase transition in the silica polymorph moganite at 570 K. Am Mineral 86(11–12):1358–1366

Heaney PJ, McKeown DA, Post JE (2007) Anomalous behavior at the I2/a to Imab phase transition in SiO$_2$-moganite: an analysis using hard-mode Raman spectroscopy. Am Mineral 92(4):631–639

Kingma KJ, Hemley RJ (1994) Raman spectroscopic study of microcrystalline silica. Am Mineral 79:269–273

Miehe G, Graetsch H (1992) Crystal structure of moganite: a new structure type of silica. Eur J Mineral 4:693–706

Miehe G, Graetsch H, Flörke OW (1984) Crystal structure and growth fabric of length-fast chalcedony. Phys Chem Miner 10(5):197–199

Miehe G, Flörke OW, Graetsch H (1986) Moganit: Strukturvorschlag für ein neues mikrokristallines SiO$_2$-mineral. Fortschritte der Mineralogie 64(Beiheft 1):117

Moxon T, Rios S (2004) Moganite and water content as a function of age in agate: an XRD and thermogravimetric study. Eur J Mineral 16(2):269–278. doi:10.1127/0935-1221/2004/0016-0269

Nash DJ, Hopkinson L (2004) A reconnaissance laser Raman and Fourier transform infrared survey of silcretes from the Kalahari Desert, Botswana. Earth Surf Proc Land 29(12):1541–1558

Rios S, Salje EKH, Redfern SAT (2001) Nanoquartz vs. macroquartz: a study of the a—ß phase transition. Eur Phys J B 20:75–83

Rodgers KA, Cressey G (2001) The occurrence, detection and significance of moganite (SiO_2) among some silica sinters. Mineral Mag 65(2):157–167

Rodgers KA, Hampton WA (2003) Laser Raman identification of silica phases comprising microtextural components of sinters. Mineral Mag 67(1):1–13. doi:10.1180/0026461036710079

Schmidt P, Fröhlich F (2011) Temperature dependent crystallographic transformations in chalcedony, SiO_2, assessed in mid infrared spectroscopy. Spectrochim Acta Part A Mol Biomol Spectrosc 78(5):1476–1481

Schmidt P, Badou A, Fröhlich F (2011) Detailed FT near-infrared study of the behaviour of water and hydroxyl in sedimentary length-fast chalcedony, SiO_2, upon heat treatment. Spectrochim Acta Part A Mol Biomol Spectrosc 81(1):552–559

Scholze H (1960) Über die quantitative UR-spektroskopische Wasserbestimmung in Silikaten. Fortschr Mineral 38(2):122–123